Published in final edited form as:
Bone. 2013 September ; 56(1): 204–212. doi:10.1016/j.bone.2013.06.003.

Fracture healing with alendronate treatment in the Brtl/+ mouse model of osteogenesis imperfecta

J.A. Meganck[a,b], **D.L. Begun**[a,b], **J.D. McElderry**[c], **A. Swick**[a,b], **K.M. Kozloff**[a,b], **S.A. Goldstein**[a,b], **M.D. Morris**[c], **J.C. Marini**[d], and **M.S. Caird**[a,*]

[a]Orthopaedic Research Laboratories, Department of Orthopaedic Surgery, University of Michigan, Ann Arbor, MI, USA

[b]Department of Biomedical Engineering, University of Michigan, Ann Arbor, MI, USA

[c]Department of Chemistry, University of Michigan, Ann Arbor, MI, USA

[d]Bone and Extracellular Matrix Branch, National Institute of Child Health and Human Development, NIH, Bethesda, MD, USA

Abstract

Osteogenesis imperfecta (OI) is a heritable bone dysplasia characterized by increased skeletal fragility. Patients are often treated with bisphosphonates to attempt to reduce fracture risk. However, bisphosphonates reside in the skeleton for many years and long-term administration may impact bone material quality. Acutely, there is concern about risk of non-union of fractures that occur near the time of bisphosphonate administration. This study investigated the effect of alendronate, a potent aminobisphosphonate, on fracture healing. Using the Brtl/+ murine model of type IV OI, tibial fractures were generated in 8-week-old mice that were untreated, treated with alendronate before fracture, or treated before and after fracture. After 2, 3, or 5 weeks of healing, tibiae were assessed using microcomputed tomography (μCT), torsion testing, quantitative histomorphometry, and Raman microspectroscopy. There were no morphologic, biomechanical or histomorphometric differences in callus between untreated mice and mice that received alendronate before fracture. Alendronate treatment before fracture did not cause a significant increase in cartilage retention in fracture callus. Both Brtl/+ and WT mice that received alendronate before and after fracture had increases in the callus volume, bone volume fraction and torque at failure after 5 weeks of healing. Raman microspectroscopy results did not show any effects of alendronate in wild-type mice, but calluses from Brtl/+ mice treated with alendronate during healing had a decreased mineral-to-matrix ratio, decreased crystallinity and an increased

*Corresponding author at: Department of Orthopaedic Surgery, University of Michigan, Mott Children's Hospital, 1540 E. Medical Center Dr., Ann Arbor, MI 48109-4241, USA., sugiyama@med.umich.edu (M.S. Caird) .
Jeff.Meganck@caliperls.com (J.A. Meganck), dbegun@umich.edu (D.L. Begun), jdmac@umich.edu (J.D. McElderry), aswick3@gmail.com (A. Swick), kenkoz@umich.edu (K.M. Kozloff), stevegld@umich.edu (S.A. Goldstein), mdmorris@umich.edu (M.D. Morris), oidoc@helix.nih.gov (J.C. Marini).

Conflict of interest

Dr. Meganck served as a consultant for GE Healthcare. Dr. Morris serves as a consultant for Kaiser optical systems. All other authors have no conflicts of interest.

Appendix A. Supplementary data

Supplementary data to this article can be found online at http://dx.doi.org/10.1016/j.bone.2013.06.003.

carbonate-to-phosphate ratio. Treatment with alendronate altered the dynamics of healing by preventing callus volume decreases later in the healing process. Fracture healing in Brtl/+ untreated animals was not significantly different from animals in which alendronate was halted at the time of fracture.

Keywords

Osteogenesis imperfecta; Bisphosphonates; Bone; Rodent; Fracture repair

Introduction

Osteogenesis imperfecta (OI) is a genetic bone dysplasia that results in increased susceptibility to fractures during childhood and adolescence. The majority of mutations that cause OI are dominant defects in the genes encoding type I collagen [1], although recessive inheritance has been described [2,3]. In most forms, these mutations cause a decrease in the amount of collagen or produce structurally abnormal type I collagen molecules and result in skeletal fragility. Most OI patients heal fractures normally [4], although there are reports of hypertrophic callus formation and delayed healing in some OI patients [5-7].

Bisphosphonates are antiresorptive medications used to treat OI patients in an effort to reduce fracture rates. These medications have been shown to be effective in reducing compression fractures in the spine [8]. A histomorphometric study of biopsies from OI patients showed increased bone formation and resorption parameters, suggesting the utility of bisphosphonate therapy in OI to control excessive bone turnover [9]. Osteoblasts and osteoclasts are both affected by bisphosphonates [10]. Bisphosphonates have a high affinity for bone mineral, and in an early assessment of alendronate, were calculated to have a half-life of over 10 years [11]. Bisphosphonate retention depends on the mechanism of delivery [12] and the rate of bone turnover. In pediatric patients, pamidronate has been detected in urine up to 8 years after cessation of treatment [13]. Furthermore, prolonged bisphosphonate treatment may play a role in abnormal bone modeling [14], radiographic metaphyseal sclerosis, osteonecrosis of the jaw, and possible accumulation of microdamage. These concerns have led to caution in bisphosphonate treatment in growing OI patients [15].

A number of clinical fracture studies with bisphosphonates have investigated the risk that disruption of underlying cellular activity with these antiresorptive agents might interfere with the normal fracture healing process. One randomized, double-blind, placebo-controlled trial with zoledronic acid following hip fracture did not show an increased risk for delayed union [16]. Similarly, in pediatric OI patients, bisphosphonate treatment is not usually associated with altered fracture healing, although intravenous pamidronate may lead to delayed osteotomy healing [17,18]. Bisphosphonate treatment is often withheld during healing following osteotomy procedures[8,19-22].

Animal studies using bisphosphonates such as alendronate, zoledronic acid, incandronate and pamidronate generally indicate an increase in callus size and structural biomechanical changes[23-30]. The biomechanical properties of the callus compared to intact bone have been shown to be similar or even improved [23,31]. With these differences in callus

mechanical properties and with concerns about impaired remodeling in the fracture healing process, fracture healing in growing OI bone in the presence of bisphosphonates was investigated.

We report here the results of a controlled fracture healing experiment with alendronate treatment using the Brtl/+ mouse model of OI. This knock-in model contains a glycine substitution mutation, models the small size and skeletal fragility that are clinical hallmarks of OI, and responds to alendronate therapy in a similar fashion to clinical patients [32-35]. Treatment groups were halted at the time of fracture or continued during healing to investigate the most common clinical options. The dynamic callus process was examined at four timepoints during healing. The primary goals were to investigate fracture healing in the Brtl/+ mouse and the impact of alendronate on regenerating tissue.

Materials and methods

Study design

All experiments were performed with IACUC approval. Male Brtl/+ mice, the progeny of Brtl/Brtl and WT parents, and male WT mice were enrolled at 2 weeks of age. For convenience of genotyping, Brtl/Brtl mice were bred with WT mice to produce Brtl+/− mice. This breeding scheme utilizes mice whose parents have distinct bone properties compared to Brtl+/− mice, which may be due to transmissible recessive effects such as gene methylation (Marini, unpublished data). The Brtl+/− mice are compared to nonlittermate WT mice generated by backcrosses in same colony. The following scheme was applied to 114 Brtl/+ mice and 133 wild type mice: the mice were randomly assigned to one of 12 experimental groups based on two variables (Fig. 1): treatment (no alendronate, alendronate before the fracture, or alendronate before and after fracture) and time of healing after fracture (1, 2, 3, 5 weeks). These time points were selected to capture the phases of fracture repair that include initial callus formation, bone formation, callus bridging, and early remodeling. All mice were weighed weekly; treated mice received alendronate 0.219 μg/g/week via subcutaneous injection (Sigma Aldrich, St. Louis, MO, USA) [35]. At 8 weeks of age, a non-locked intramedullary pin was placed in an antegrade manner in one randomly selected tibia and a fracture was generated with a guillotine drop weight method in the mid-tibia [36]. The fracture pattern was categorized on post-operative radiographs as simple, wedge, or comminuted according to the classification system of the Orthopaedic Trauma Association [37]. After the period of healing, euthanasia was performed and intact and fractured tibiae were dissected and prepared for analysis.

Microcomputed tomography

All specimens underwent μCT analysis. Tibiae were scanned using a commercially available μCT system (eXplore Locus SP, GE Healthcare Preclinical Imaging) [38] using a source voltage of 80 kVp, a source current of 80 μA, 2 × 2 detector binning and an exposure time of 1600 ms. The raw data were corrected with bright and dark pixel corrections and a sinogram based filter, and were reconstructed using a Feldkamp cone beam backprojection algorithm to obtain images with an 18 μm isotropic voxel size. The callus volume, bone volume fraction (BVF) and tissue mineral density (TMD) of bone in the callus and residual cortical

bone were measured (MicroView 2.2, GE Healthcare Preclinical Imaging) [36]. Briefly, a spline based semi-automatic segmentation was used to define the outer callus boundary. A second spline based segmentation in combination with a threshold-confined region growing procedure was used to select the cortical bone. A Boolean operation was then performed on these two segmentations to create a region which only included bone in the callus. This region also included the intramedullary space because healing bone was present in the marrow cavity as well.

Biomechanical testing

A randomly assigned subset of the fractured tibiae and contralateral intact controls was tested in torsion [36]. Whole bone specimens were potted using low melting temperature solder, mounted in a custom torsion tester interfaced with LabView, wetted with saline, and tested in external rotation at 0.5°/s until failure. Using a MATLAB script, raw data were filtered and stiffness, angular displacement at failure, torque at failure, and energy to failure were measured.

Quantitative histology

Fractured tibiae were fixed, decalcified, embedded in paraffin, and sectioned at 7 μm. The slides were stained using (1) Safranin-O, Fast Green and Hematoxylin to assess cartilage, (2) tartrate-resistant acid phosphatase (387A, Sigma Aldrich, St. Louis, MO, USA) to assess osteoclasts or (3) picrosirius red for subsequent collagen analyses.

To analyze the Safranin-O stained slides, a custom ImageJ macro based on a color deconvolution technique was used to separate the Safranin-O component from the Fast Green and Hematoxylin components [39]. This macro was implemented to assess both the amount of cartilage within the callus tissue and the trabeculated bone of the callus [40].

TRAP analyses were performed on fractured tibiae from mice that healed for 5 weeks. Osteoclast number per bone surface (OcN/BS) and osteoclast surface per bone surface (OcS/BS) were measured on the periosteal surface of both the anterior and posterior callus using commercially available software (BioQuant, Nashville, TN, USA).

To analyze picrosirius red stained slides, a polarized light method was implemented based on previously published techniques [41,42]. Briefly, a rotating stage was placed on a standard light microscope (Olympus BX-51). A linear polarizer was placed between the light source and stage and was crossed with a linearly oriented analyzer between the objective and camera. The section was placed on the stage, defining 0° to align with the longitudinal axis of the bone. The stage was then rotated in increments of 5 or 10° and images were captured at each stage rotation. These images were then imported into MATLAB and, using a custom script combined with the ImageJ TurboReg plugin, the images for each orientation were registered. This facilitated analysis of the polarized light images on a pixel by pixel basis. These images were segmented and thresholded to analyze the trabeculated bone of the callus separately from the residual cortical bone. The parallelism index (PI), a measure of collagen alignment [41], was calculated for residual cortical bone and the trabeculated bone of the healing callus. A high PI indicates the collagen fibrils are organized in a parallel manner, whereas unorganized fibrils have a low

PI. PI is the (maximum intensity − minimum intensity)/(maximum intensity + minimum intensity). Polarized light analysis was performed for untreated mice after 5 weeks of healing.

Raman microspectroscopy

Raman spectra were acquired on a custom microprobe system, described previously [43] functioning in the near-IR (785-nm excitation) with a 20 × 0.75NA objective. Whole harvested isolated tibiae were thawed, placed in a Petri dish, and kept moist with PBS. Ten spectra were acquired from the central portion of the callus or tibial mid-diaphysis for contralateral intact control limbs.

Spectra were normalized to the height of the phenylalanine ring (~1002 cm^{-1}). Four separate outcome measurements were made. Crystallinity (or crystal size and perfection) was measured as the inverse full width at half height of the 960 cm^{-1} peak [44]. The carbonate-to-phosphate ratio was calculated as the ratio of band areas for the 1070 cm^{-1} to 960 cm^{-1} peak [45]. The cross-linking ratio was calculated in the Amide I band by applying a five-peak fit (1630, 1645, 1660, 1675 and 1690 cm^{-1}) and measuring the ratio of the area under the 1660 band to the area under the 1690 band[45-47]. This metric, extended from on FTIR based techniques [47], has been utilized to estimate the degree of collagen cross-linking[45,46]. However, the method is not validated.

Mineral-to-matrix ratios were estimated using three different metrics. These were the area of the 960 cm^{-1} band relative to the peak areas representing hydroxyproline and proline (851, 873 and 917 cm^{-1}) [48], the height of the 960 cm^{-1} peak relative to the height of the CH_2 wag peak (1445 cm^{-1}) [45], and the area of the 960 cm^{-1} peak relative to the area under the Amide I band [46]. When peak fitting was required, a custom MATLAB script was implemented using the Levenberg–Marquardt method of curve fitting using mixed Gaussian–Lorentzian functions.

To determine whether spectroscopic measurements at the periosteal surface were representative, a subset of tibiae from untreated mice (n = 4 Brtl/+, n = 5 WT) was sectioned longitudinally for Raman mapping of the cross section at the mid-diaphysis. Tibiae were kept fresh-frozen (not embedded or fixed) while glued to a microscope slide for support and hand polished using fine polishing paper (1200–3000 grit). The polished cortical bone surface was sufficiently flat and smooth for imaging under 20× magnification. Spectra nearest the surface (15 μm from the edge) were classified as surface measurements. A histogram of the surface spectra was compared with a histogram of the spectra through the cross section.

Statistical analysis

Results of the torsion biomechanical testing and μCT analysis were examined using analysis of covariance (ANCOVA) models to assess changes in the three main effects (genotype, alendronate treatment protocol, and duration of healing) and their interactions using weight, fracture complexity, and gage length as covariates. Post-hoc comparisons were only applied to main effects controlling for covariates gage length and weight (Supplementary Table 1). The sample sizes for each group ranged from 4 to 18 (Supplementary Tables 2-4).

A full factorial 2-way analysis of variance (ANOVA) was used to test for differences between treatments and genotypes for the TRAP slides, Safranin-O/Fast Green slides, and the picrosirius red slides. The difference between the polarized light metrics for cortical bone between the Brtl/+ and WT mice were compared using a t-test to assess collagen orientation.

Raman microspectroscopy data were analyzed using a two-step approach. First, the intraclass correlation coefficient was calculated to determine the variance between samples (n = 6–7 per group) compared to the variance of the 10 spectra within each bone. These results indicated correlations that were reasonable (ranging from 0.514 to 0.759) for all variables except the cross-linking ratio, so these 10 measurements were averaged to obtain one measurement per metric for each specimen. Second, a 2-way ANOVA was applied to the aggregated data for each limb and each variable to look for changes between the genotypes and alendronate treatment. Post-hoc tests using a Bonferroni correction looked for significant pairwise differences.

Results

Study design and animal model

In this analysis, 67% had simple fractures, 12% had wedge fractures, 18% had comminuted fractures, and 3% could not be assigned radiographically. Fracture complexity did not differ between the Brtl/+ and WT mice. Brtl/+ mice weighed less than their WT counterparts and, consistent with previous data [35], the weight gain was not affected by alendronate treatment.

Microcomputed tomography

247 mice underwent μCT analysis with 12 to 18 mice per group (Supplementary Table 2). Review of μCT images of intact tibiae from mice with one week of healing showed bands of mineralized cartilage in mice that received alendronate, but in the fractured tibiae at one week there was not enough mineral to detect the callus boundary. Fractured tibiae from mice that healed for 2, 3 and 5 weeks had sufficient mineral to detect the callus boundary and were scanned by μCT. ANOVA analyses did not indicate any significant 3-way interactions between the duration of healing, alendronate protocol and genotype (results not shown). There were no measureable differences between treatment groups in the callus volume, bone volume fraction, or tissue mineral density of bone in the callus after 2 weeks of healing when genotypes were pooled (Fig. 2). Mice treated with alendronate throughout fracture repair had an increased callus BVF compared to untreated or alendronate until fracture groups at 3 weeks (Fig. 2B) and increased callus volume and BVF at 5 weeks of healing (Figs. 2A, B). These changes in callus morphology and volume fraction were subjectively noticeable when viewing the μCT images of fracture calluses after 5 weeks of healing (Fig. 3A). Neither the genotype nor alendronate treatment protocols affected callus mineralization. In pooled data, TMD increased in callus bone from 2 weeks to 3 weeks, and again from 3 weeks to 5 weeks (Fig. 2C), although even after 5 weeks the trabecular mineral density was still far less than the residual cortical bone.

Biomechanical testing

136 mice underwent biomechanical testing with 4–12 final specimens per group. Numbers differed because some of the samples were lost in the groups at different steps during the experiment. Fractured tibiae from mice that healed for 2, 3, and 5 weeks were tested biomechanically. The angular displacement to failure decreased from 2 to 3 weeks of healing. Additionally, the stiffness, energy to failure, and torque to failure increased from 2 to 3 weeks (data not shown) and again from 3 to 5 weeks (Fig. 4).

After 2 weeks of healing there were no changes in angular displacement at failure in animals treated with alendronate during healing compared to the other treatment groups ($p = 0.076$; data not shown). After 3 weeks in WT but not Brtl/+ mice with continued alendronate treatment, there was a decrease in stiffness in comparison to untreated (Fig. 4A). Untreated Brtl/+ mice had decreased callus stiffness compared to all treatment groups of WT mice, but no effect of treatment was found (Fig. 4A). After 3 weeks, the combined Brtl/+ treatment groups but not WT had decreased energy to failure and ultimate torque (Figs. 4B, C). After 5 weeks of healing, fracture calluses from WT but not Brtl/+ mice that received continued alendronate treatment showed increased stiffness compared to untreated (Fig. 4D). When the genotypes were pooled for analysis after 5 weeks, treatment during healing was associated with increased torque at failure (Figs. 4E, F).

Intact tibiae demonstrated differences with respect to treatment protocol. Animals that received 3 weeks of alendronate injections displayed an increased torque at failure compared to halted or untreated animals. When the effects of time and alendronate treatment were pooled, Brtl/+ tibiae showed reductions in stiffness, angular displacement to failure, torque at failure and energy to failure compared to WT. After 5 weeks, there was no statistically significant change in energy to failure between the fractured and intact tibiae of WT mice but the fractured tibiae of Brtl/+ mice had a significant increase compared to the contralateral intact tibiae (Fig. 5), suggesting that callus is stronger than bone in Brtl/+ mice but not in WT.

Quantitative histology

111 mice underwent histologic evaluation. Safranin-O/Fast Green stained sections revealed cartilage in the callus through 2 weeks of healing, but none by 3 weeks. Neither the genotype nor the alendronate treatment protocol had an impact on the amount of cartilage present in the callus. There was also no detectable change in the percentage of cartilage that contained trabeculated woven bone after alendronate treatment.

To better understand the increased energy to failure in the fracture callus compared to intact tibiae in Brtl/+ mice after 5 weeks of healing, polarized light analysis was used to study collagen structure. Comparison of mean intensity versus stage angle indicated that collagen was oriented differently in callus and the residual cortical bone in both genotypes, implying that bone in the callus is more woven in nature. The parallelism index (PI) for callus bone was significantly lower than for residual cortical bone, verifying the woven nature of this mineralized tissue (Fig. 6).

The μCT data indicated an effect of alendronate treatment on callus volume after 5 weeks of healing with continued alendronate. However, TRAP analysis performed at the periosteal callus boundary of animals that healed for 5 weeks did not indicate an effect of genotype or alendronate treatment on the osteoclast surface per bone surface or in the number of osteoclasts by 2-way ANOVA.

Raman microspectroscopy

Raman microspectroscopy was performed on the fracture calluses and the contralateral intact tibiae from mice that healed for 3 weeks. Within a genotype, the alendronate treatment protocol did not affect the crystallinity, mineral-to-matrix ratio or carbonate-to-phosphate ratio (Fig. 7A). There were no changes in cross-linking ratio with treatment or between genotypes (data not shown). When no alendronate was administered, mineral in both the intact and fractured tibiae of Brtl/+ mice had decreased crystallinity compared to WT, and the fractured tibiae had an increased carbonate-to-phosphate ratio (Fig. 7A). When alendronate treatment was continued during healing, fractured tibiae from Brtl/+ mice had a decreased mineral-to-matrix ratio, and the mineral had a decreased crystallinity and an increased carbonate-to-phosphate ratio (Fig. 7A). Scatterplots revealed a positive correlation between crystallinity and the mineral-to-matrix ratio (Fig. 7B) and a similar negative correlation between the crystallinity and the carbonate-to-phosphate ratio. Spectra were obtained through the cross section to ensure that these results were not biased by restricting measurements to the periosteal surface. Measurements for all samples were combined together in histograms for spectra taken at the surface which appear to be a reasonable sampling of spectra taken through the cortical thickness (Fig. 7C).

Discussion

Patients with OI are treated with bisphosphonates to attempt to decrease fracture risk. If a fracture does occur in a patient on bisphosphonate therapy, questions have been raised about the theoretical risk of non-union or delay in fracture healing. This study used the Brtl/+ knock-in mouse model of OI to address the question of early fracture healing in the context of bisphosphonate therapy. Continued alendronate treatment throughout healing prevented the normal remodeling of the callus between 3 and 5 weeks. The resulting larger callus and increased bone volume fraction may account for the observed increase in torque at failure in the continued therapy group compared to the group for which therapy was halted at the time of fracture. Similar findings have been observed when bisphosphonate was given during fracture repair in other animal models [24-28,30].

When alendronate treatment was halted at fracture, very subtle alterations in healing were observed compared to untreated groups. This corroborates previous studies that indicate halting bisphosphonate treatment at the time of fracture did not result in a change in callus size or structural biomechanical properties [24,31]. In these studies, there were no differences in bisphosphonate concentration between the callus and cortical bone [24] suggesting that no additional bisphosphonate was incorporated into the callus during fracture repair following treatment cessation. However, when bisphosphonates were given during fracture repair, drug concentration was shown to localize highly within the callus through

radiologic and fluorescent imaging modalities[24,49]. In the present study, as in previously published results [35], there were noticeable bands of mineralized cartilage in the metaphyses of mice that received alendronate (Fig. 3B). These bands correlate with the number, frequency, and spacing of drug cycles [50], and coincide with regions of high local bisphosphonate concentration [51].

To monitor osteoclast dynamics during fracture healing, TRAP staining was performed after 5 weeks of tissue repair. While previous data show an inherent increase in osteoclast number in untreated Brtl/+ compared to WT [34], no differences in the number of osteoclasts or in the osteoclast surface per bone surface were observed between the genotypes or the treatment groups in the present study. Fracture healing is a dynamic process, and others have noted distinct increases [30], decreases [24,25] and no change [27] in osteoclast number or surface with bisphosphonate therapy during fracture repair. These changes likely differ based on animal model, fracture technique, and time of observation following injury. While these disparities make a true interpretation difficult, it seems plausible that the fracture healing dynamics after 5 weeks of healing in this study supersede any potential treatment and genotype effects. Alternatively, since we studied only the periosteal callus surface, treatment and genotype effects may be more pronounced on the interior of the callus.

To investigate this question in more depth, transient changes during healing were assessed. The energy to failure in fracture calluses from untreated Brtl/+ mice was significantly increased in comparison to the contralateral intact tibia after 5 weeks of healing. This can partially be attributed to the callus being larger than the intact tibia. In addition, we investigated collagen orientation in fracture callus and residual cortical bone using polarized light studies of untreated Brtl/+ mice. Similar to previously published studies [52], bone in the callus was less organized and more woven than cortical bone (Fig. 5). The magnitude of this change in collagen orientation is far greater than any subtle difference between genotypes and, therefore, may govern the biomechanics during healing. However, fractured bones in *oim/oim* mice did not have increased structural properties in comparison to the contralateral intact bones [53], so this result may be specific to bone with heterotrimeric collagen.

Other transient changes were also investigated during healing. Between 2 and 3 weeks of healing, the stiffness of the callus increased and the angular displacement to failure decreased. This is consistent with the transition from cartilage at the callus center to a bridged bony callus that was seen histologically. Therefore, 3 weeks was the earliest healing timepoint when the calluses were bridged and carti-lage was removed.

Raman microspectroscopy was performed to investigate changes at this 3-week timepoint that may underlie the morphologic and functional changes seen after 5 weeks of healing. The Raman analysis did not indicate any effect of alendronate treatment at the peripheral callus boundary and the periosteal surface of the intact bone. The mice were euthanized 1 week after the last alendronate injection so, if there are spatial dependencies based on the presence of alendronate in circulation during bone formation, these surfaces may not have detected it. Comparison of the Raman results between the genotypes supports this possibility. The crystallinity differences seem to correlate to a change in mineral-to-matrix

ratio, possibly implying that crystallinity changes with localized mineral deposition. There were no detectable changes in cross-linking, although this is the most difficult metric to assess due to the high variation of measurements within a bone. Although this method lacks validation, reported correlations between IR and Raman spectroscopy are R^2 in the 0.8–0.85 range largely because the Raman data are generally noisier than IR data [54].

This study has several limitations. First, the breeding scheme (Brtl/Brtl × WT) which was chosen to minimize genotyping of pups and Brtl/+ lethality [32] may have resulted in transmission of recessive traits at noncollagenous loci. The persistence in our Brtl/+ pups of decreased weight and bone density as well as femoral biomechanical traits suggest that the mating scheme did not significantly interfere with interpretation of the data. Second, the control mice did not receive saline injections. However, they were handled weekly for weighing, which did cause mild stress which is roughly comparable to the simple subcutaneous injections received by treated mice. Third, the ANCOVA statistical analysis used weight as a proxy for bone size when analyzing biomechanical data; this allowed simultaneous analysis of the fractured and intact tibiae, but the assumption may have introduced error into the biomechanical analysis. Last, although four timepoints were analyzed to encompass the range of ossification and early remodeling in fracture healing dynamics, late remodeling dynamics were not directly examined. Investigations that look at later timepoints are required to determine whether fracture calluses from mice treated with alendronate during healing will ever remodel and return to a normal cortical morphology.

Conclusions

Fracture calluses contain woven bone that appears to override the biomechanical deficiencies inherent in intact bones from Brtl/+ mice. Treating these mice with alendronate during fracture healing resulted in larger calluses with increased structural biomechanical properties, although it altered the dynamics of healing by preventing callus volume decreases later in the healing process. These murine results suggest that a complex situation would occur in OI patients given bisphosphonates during fracture healing. On the one hand, the geometric advantage we described may help reduce the inherent risk of re-fracture during the healing process. On the other hand, the larger callus will contain increased bisphosphonate concentrations and the kinetics of callus resolution may be delayed.

Supplementary Material

Refer to Web version on PubMed Central for supplementary material.

Acknowledgments

The authors would like to thank Bonnie Nolan, Kathy Sweet, Sharon Reske, Xixi Wang, Jason Combs, Dennis Kayner, and Charles Roehm. Thanks also to Lingling Zhang for statistical support. The authors would also like to acknowledge support from the National Science Foundation Graduate Research Fellowship Program (JAM), the University of Michigan Musculoskeletal Core Center (SAG; NIH AR46024), the regenerative sciences training grant (SAG; NIH T90 DK070071), the University of Michigan Department of Orthopaedic Surgery (MSC), the National Institutes of Health (MDM; R01 AR047969), and NICHD Intramural Funding (JCM). These funding sources did not have involvement in the study design; collection, analysis, or interpretation of data; or in the report or its publication submission.

References

[1]. Marini JC, Forlino A, Cabral WA, Barnes AM, San Antonio JD, Milgrom S, et al. Consortium for osteogenesis imperfecta mutations in the helical domain of type I collagen: regions rich in lethal mutations align with collagen binding sites for integrins and proteoglycans. Hum Mutat. 2007; 28(3):209–21. [PubMed: 17078022]

[2]. Baldridge D, Schwarze U, Morello R, Lennington J, Bertin TK, Pace JM, et al. CRTAP and LEPRE1 mutations in recessive osteogenesis imperfecta. Hum Mutat. 2008; 29(12):1435–42. [PubMed: 18566967]

[3]. Marini JC, Cabral WA, Barnes AM, Chang W. Components of the collagen prolyl 3-hydroxylation complex are crucial for normal bone development. Cell Cycle. 2007; 6(14):1675–81. [PubMed: 17630507]

[4]. Herring, JA.; Tachdjian, MO., editors. Tachdjian's Pediatric Orthopaedics. 3rd ed. Vol. 3. W.B. Saunders; Philadelphia: 2002.

[5]. Cheung MS, Glorieux FH, Rauch F. Natural history of hyperplastic callus formation in osteogenesis imperfecta type V. J Bone Miner Res. 2007; 22(8):1181–6. [PubMed: 17451374]

[6]. Ramirez N, Vilella FE, Colon M, Flynn JM. Osteogenesis imperfecta and hyperplastic callus formation in a family: a report of three cases and a review of the literature. J Pediatr Orthop B. 2003; 12(2):88–96. [PubMed: 12584490]

[7]. Alharbi M, Pinto G, Finidori G, Souberbielle JC, Guillou F, Gaubicher S, et al. Pamidronate treatment of children with moderate-to-severe osteogenesis imperfecta: a note of caution. Horm Res. 2009; 71(1):38–44. [PubMed: 19039235]

[8]. Letocha AD, Cintas HL, Troendle JF, Reynolds JC, Cann CE, Chernoff EJ, et al. Controlled trial of pamidronate in children with types III and IV osteogenesis imperfecta confirms vertebral gains but not short-term functional improvement. J Bone Miner Res. 2005; 20(6):977–86. [PubMed: 15883638]

[9]. Rauch F, Travers R, Parfitt AM, Glorieux FH. Static and dynamic bone histomorphometry in children with osteogenesis imperfecta. Bone. 2000; 26(6):581–9. [PubMed: 10831929]

[10]. Russell RG, Watts NB, Ebetino FH, Rogers MJ. Mechanisms of action of bisphosphonates: similarities and differences and their potential influence on clinical efficacy. Osteoporos Int. 2008; 19(6):733–59. [PubMed: 18214569]

[11]. Gertz BJ, Holland SD, Kline WF, Matuszewski BK, Porras AG. Clinical pharmacology of alendronate sodium. Osteoporos Int. 1993; 3(Suppl. 3):S13–6. [PubMed: 8298197]

[12]. Ward LM, Denker AE, Porras A, Shugarts S, Kline W, Travers R, et al. Single-dose pharmacokinetics and tolerability of alendronate 35- and 70-milligram tablets in children and adolescents with osteogenesis imperfecta type I. J Clin Endocrinol Metab. 2005; 90(7):4051–6. [PubMed: 15827104]

[13]. Papapoulos SE, Cremers SC. Prolonged bisphosphonate release after treatment in children. N Engl J Med. 2007; 356(10):1075–6. [PubMed: 17347467]

[14]. Whyte MP, McAlister WH, Novack DV, Clements KL, Schoenecker PL, Wenkert D. Bisphosphonate-induced osteopetrosis: novel bone modeling defects, metaphyseal osteopenia, and osteosclerosis fractures after drug exposure ceases. J Bone Miner Res. 2008; 23(10):1698–707. [PubMed: 18505375]

[15]. Marini JC. Bone: Use of bisphosphonates in children-proceed with caution. Nat Rev Endocrinol. 2009; 5(5):241–3. [PubMed: 19444252]

[16]. Lyles KW, Colon-Emeric CS, Magaziner JS, Adachi JD, Pieper CF, Mautalen C, et al. Zoledronic acid and clinical fractures and mortality after hip fracture. N Engl J Med. 2007; 357(18):1799–809. [PubMed: 17878149]

[17]. Munns CF, Rauch F, Zeitlin L, Fassier F, Glorieux FH. Delayed osteotomy but not fracture healing in pediatric osteogenesis imperfecta patients receiving pamidronate. J Bone Miner Res. 2004; 19(11):1779–86. [PubMed: 15476577]

[18]. Pizones J, Plotkin H, Parra-Garcia JI, Alvarez P, Gutierrez P, Bueno A, et al. Bone healing in children with osteogenesis imperfecta treated with bisphosphonates. J Pediatr Orthop. 2005; 25(3):332–5. [PubMed: 15832149]

[19]. Rauch F, Glorieux FH. Osteogenesis imperfecta. Lancet. 2004; 363(9418):1377–85. [PubMed: 15110498]

[20]. Gatti D, Antoniazzi F, Prizzi R, Braga V, Rossini M, Tato L, et al. Intravenous neridronate in children with osteogenesis imperfecta: a randomized controlled study. J Bone Miner Res. 2005; 20(5):758–63. [PubMed: 15824848]

[21]. Rauch F, Munns CF, Land C, Cheung M, Glorieux FH. Risedronate in the treatment of mild pediatric osteogenesis imperfecta: a randomized placebo-controlled study. J Bone Miner Res. 2009; 24(7):1282–9. [PubMed: 19257821]

[22]. Sakkers R, Kok D, Engelbert R, van Dongen A, Jansen M, Pruijs H, et al. Skeletal effects and functional outcome with olpadronate in children with osteogenesis imperfecta: a 2-year randomised placebo-controlled study. Lancet. 2004; 363(9419):1427–31. [PubMed: 15121405]

[23]. Peter CP, Cook WO, Nunamaker DM, Provost MT, Seedor JG, Rodan GA. Effect of alendronate on fracture healing and bone remodeling in dogs. J Orthop Res. 1996; 14(1):74–9. [PubMed: 8618170]

[24]. Li J, Mori S, Kaji Y, Kawanishi J, Akiyama T, Norimatsu H. Concentration of bisphosphonate (incadronate) in callus area and its effects on fracture healing in rats. J Bone Miner Res. 2000; 15(10):2042–51. [PubMed: 11028459]

[25]. Cao Y, Mori S, Mashiba T, Westmore MS, Ma L, Sato M, et al. Raloxifene, estrogen, and alendronate affect the processes of fracture repair differently in ovariectomized rats. J Bone Miner Res. 2002; 17(12):2237–46. [PubMed: 12469918]

[26]. Amanat N, Brown R, Bilston LE, Little DG. A single systemic dose of pamidronate improves bone mineral content and accelerates restoration of strength in a rat model of fracture repair. J Orthop Res. 2005; 23(5):1029–34. [PubMed: 16140188]

[27]. Amanat N, McDonald M, Godfrey C, Bilston L, Little D. Optimal timing of a single dose of zoledronic acid to increase strength in rat fracture repair. J Bone Miner Res. 2007; 22(6):867–76. [PubMed: 17371160]

[28]. Greiner SH, Wildemann B, Back DA, Alidoust M, Schwabe P, Haas NP, et al. Local application of zoledronic acid incorporated in a poly(D, l-lactide)-coated implant accelerates fracture healing in rats. Acta Orthop. 2008; 79(5):717–25. [PubMed: 18839381]

[29]. McDonald MM, Dulai S, Godfrey C, Amanat N, Sztynda T, Little DG. Bolus or weekly zoledronic acid administration does not delay endochondral fracture repair but weekly dosing enhances delays in hard callus remodeling. Bone. 2008; 43(4):653–62. [PubMed: 18582604]

[30]. Gerstenfeld LC, Sacks DJ, Pelis M, Mason ZD, Graves DT, Barrero M, et al. Comparison of effects of the bisphosphonate alendronate versus the RANKL inhibitor denosumab on murine fracture healing. J Bone Miner Res. 2009; 24(2):196–208. [PubMed: 19016594]

[31]. Li J, Mori S, Kaji Y, Mashiba T, Kawanishi J, Norimatsu H. Effect of bisphosphonate (incadronate) on fracture healing of long bones in rats. J Bone Miner Res. 1999; 14(6):969–79. [PubMed: 10352106]

[32]. Forlino A, Porter FD, Lee EJ, Westphal H, Marini JC. Use of the Cre/lox recombination system to develop a non-lethal knock-in murine model for osteogenesis imperfecta with an alpha1(I) G349C substitution variability in phenotype in BrtlIV mice. J Biol Chem. 1999; 274(53):37923–31. [PubMed: 10608859]

[33]. Kozloff KM, Carden A, Bergwitz C, Forlino A, Uveges TE, Morris MD, et al. Brittle IV mouse model for osteogenesis imperfecta IV demonstrates postpubertal adaptations to improve whole bone strength. J Bone Miner Res. 2004; 19(4):614–22. [PubMed: 15005849]

[34]. Uveges TE, Collin-Osdoby P, Cabral WA, Ledgard F, Goldberg L, Bergwitz C, et al. Cellular mechanism of decreased bone in Brtl mouse model of OI: imbalance of decreased osteoblast function and increased osteoclasts and their precursors. J Bone Miner Res. 2008; 23(12):1983–94. [PubMed: 18684089]

[35]. Uveges TE, Kozloff KM, Ty JM, Ledgard F, Raggio CL, Gronowicz G, et al. Alendronate treatment of the brtl osteogenesis imperfecta mouse improves femoral geometry and load response before fracture but decreases predicted material properties and has detrimental effects on osteoblasts and bone formation. J Bone Miner Res. 2009; 24(5):849–59. [PubMed: 19113917]

[36]. Taylor DK, Meganck JA, Terkhorn S, Rajani R, Naik A, O'Keefe RJ, et al. Thrombospondin-2 influences the proportion of cartilage and bone during fracture healing. J Bone Miner Res. 2009; 24(6):1043–54. [PubMed: 19123916]

[37]. Fracture and dislocation compendium. Orthopaedic Trauma Association Committee for Coding and Classification. J Orthop Trauma. 1996; 10(Suppl. 1):v–ix. 1–154. [PubMed: 8814583]

[38]. Meganck JA, Kozloff KM, Thornton MM, Broski SM, Goldstein SA. Beam hardening artifacts in micro-computed tomography scanning can be reduced by X-ray beam filtration and the resulting images can be used to accurately measure BMD. Bone. 2009; 45(6):1104–16. [PubMed: 19651256]

[39]. Ruifrok AC, Johnston DA. Quantification of histochemical staining by color deconvolution. Anal Quant Cytol Histol. 2001; 23(4):291–9. [PubMed: 11531144]

[40]. Smith EJ, McEvoy A, Little DG, Baldock PA, Eisman JA, Gardiner EM. Transient retention of endochondral cartilaginous matrix with bisphosphonate treatment in a long-term rabbit model of distraction osteogenesis. J Bone Miner Res. 2004; 19(10):1698–705. [PubMed: 15355565]

[41]. Rieppo J, Hallikainen J, Jurvelin JS, Kiviranta I, Helminen HJ, Hyttinen MM. Practical considerations in the use of polarized light microscopy in the analysis of the collagen network in articular cartilage. Microsc Res Tech. 2008; 71(4):279–87. [PubMed: 18072283]

[42]. Silva MJ, Brodt MD, Wopenka B, Thomopoulos S, Williams D, Wassen MH, et al. Decreased collagen organization and content are associated with reduced strength of demineralized and intact bone in the SAMP6 mouse. J Bone Miner Res. 2006; 21(1):78–88. [PubMed: 16355276]

[43]. Carden A, Rajachar RM, Morris MD, Kohn DH. Ultrastructural changes accompanying the mechanical deformation of bone tissue: a Raman imaging study. Calcif Tissue Int. 2003; 72(2): 166–75. [PubMed: 12469250]

[44]. Kazanci M, Fratzl P, Klaushofer K, Paschalis EP. Complementary information on in vitro conversion of amorphous (precursor) calcium phosphate to hydroxyapatite from Raman microspectroscopy and wide-angle X-ray scattering. Calcif Tissue Int. 2006; 79(5):354–9. [PubMed: 17120187]

[45]. Dehring KA, Crane NJ, Smukler AR, McHugh JB, Roessler BJ, Morris MD. Identifying chemical changes in subchondral bone taken from murine knee joints using Raman spectroscopy. Appl Spectrosc. 2006; 60(10):1134–41. [PubMed: 17059665]

[46]. Wallace JM, Golcuk K, Morris MD, Kohn DH. Inbred strain-specific response to biglycan deficiency in the cortical bone of C57BL6/129 and C3H/He mice. J Bone Miner Res. 2009; 24(6):1002–12. [PubMed: 19113913]

[47]. Paschalis EP, Verdelis K, Doty SB, Boskey AL, Mendelsohn R, Yamauchi M. Spectroscopic characterization of collagen cross-links in bone. J Bone Miner Res. 2001; 16(10):1821–8. [PubMed: 11585346]

[48]. Kohn DH, Sahar ND, Wallace JM, Golcuk K, Morris MD. Exercise alters mineral and matrix composition in the absence of adding new bone. Cells Tissues Organs. 2009; 189(1-4):33–7. [PubMed: 18703871]

[49]. Kozloff KM, Weissleder R, Mahmood U. Noninvasive optical detection of bone mineral. J Bone Miner Res. 2007; 22(8):1208–16. [PubMed: 17488196]

[50]. Al Muderis M, Azzopardi T, Cundy P. Zebra lines of pamidronate therapy in children. J Bone Joint Surg Am. 2007; 89(7):1511–6. [PubMed: 17606790]

[51]. Kozloff, KM.; Sinder, BP.; Caird, MS. Transactions of the 56th annual meeting of the Orthopaedic Research Society (New Orleans, LA). Orthopaedic Research Society; Rosemont, IL: 2010. Spatial heterogeneity of bisphosphonate delivery and retention influences local healing of bone in model of disuse osteopenia; p. 461

[52]. Tonna EA. Fracture callus formation in young and old mice observed with polarized light microscopy. Anat Rec. 1964; 150:349–61. [PubMed: 14248305]

[53]. Delos D, Yang X, Ricciardi BF, Myers ER, Bostrom MP, Camacho NP. The effects of RANKL inhibition on fracture healing and bone strength in a mouse model of osteogenesis imperfecta. J Orthop Res. 2008; 26(2):153–64. [PubMed: 17729310]

[54]. Gourion-Arsiquaud S, Burket JC, Havill LM, DiCarlo E, Doty SB, Mendelsohn R, et al. Spatial variation in osteonal bone properties relative to tissue and animal age. J Bone Miner Res. 2009; 24(7):1271–81. [PubMed: 19210217]

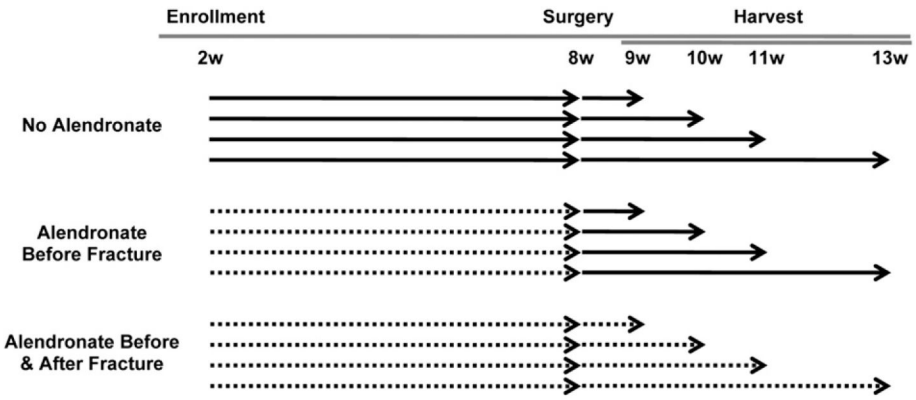

Fig. 1.

Study design. Solid arrows indicate when no alendronate injections were given. Dashed lines indicate when weekly subcutaneous injections of alendronate were given. The following groups were tested for both Brtl/+ and wild type (WT) mice.

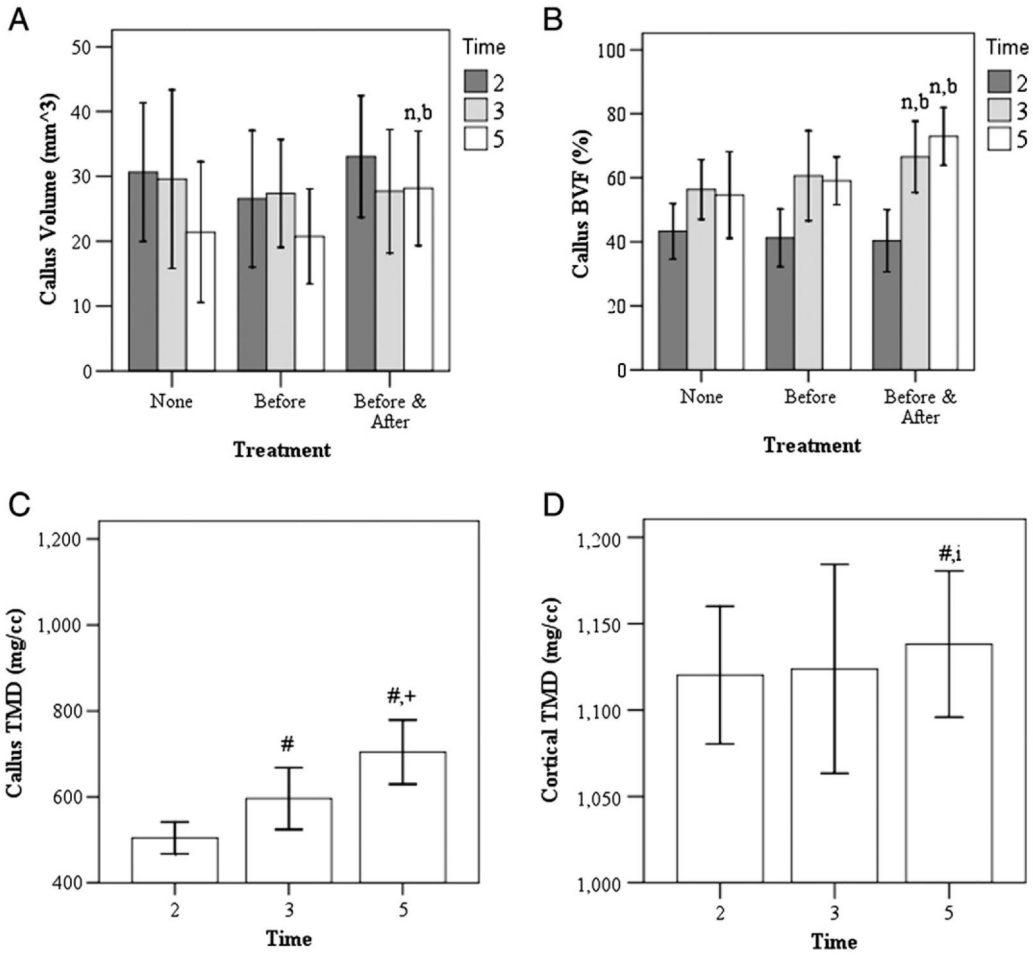

Fig. 2.

Quantitative microcomputed tomography results for callus morphology and densitometry for pooled genotype data. (A) Callus volume and (B) bone volume fraction during healing. Tissue mineral densities (TMD) for the (C) bone in the callus and (D) residual cortical bone. Notations indicate significance (p b 0.05) with respect to no alendronate treatment (n), alendronate treatment before fracture (b) in parts A and B. Notations indicate significance ($p < 0.05$) with respect to 2 weeks of healing (#) or 3 weeks of healing (+) in parts C and D; i, $p = 0.064$.

Fig. 3.

Representative sagittal planes of microcomputed tomography images from (A) WT mice after 5 weeks of healing and (B) from the intact tibiae of 9-week-old mice. “None” represents no alendronate treatment, “Before” is alendronate before fracture, and “Continued” is treatment before and after fracture.

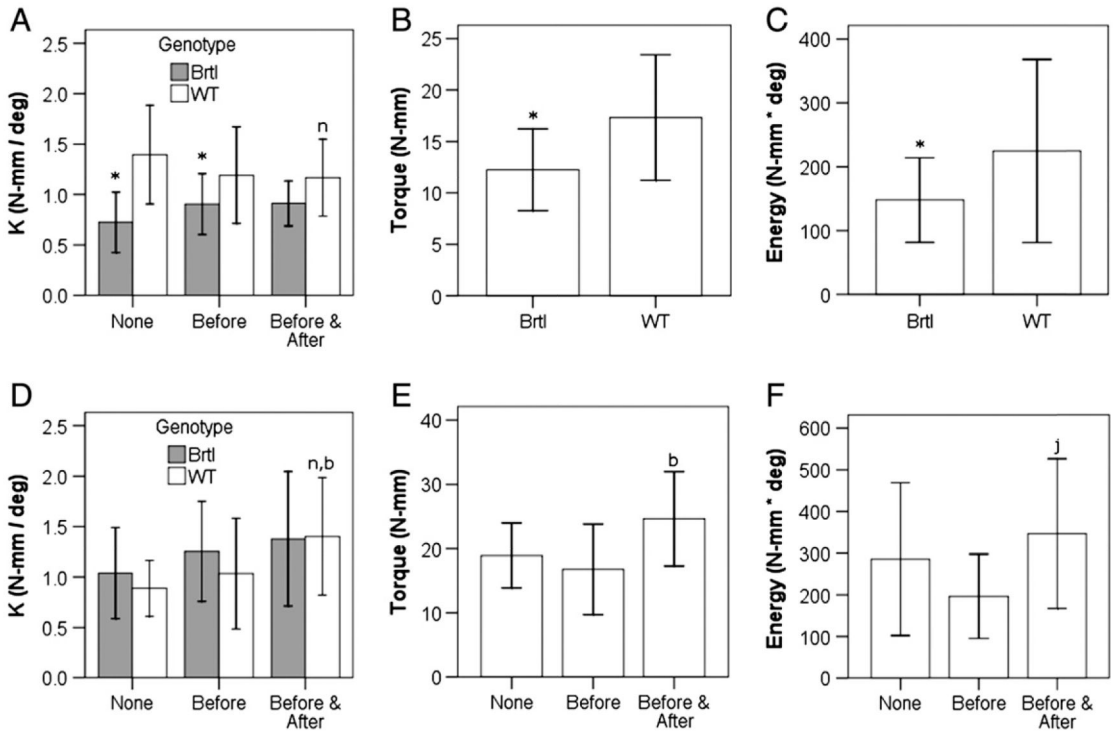

Fig. 4.

Biomechanical changes in fracture calluses based on genotypic and treatment protocol variations at 3 weeks of healing (A–C) and 5 weeks of healing (D–F). Stiffness (A, D), torque at failure (B, E) and energy to failure (C, F) are shown. Notations indicate significance ($p < 0.05$) with respect to no alendronate treatment (n), alendronate treatment before fracture (b), or between the genotypes (*). In (F), mice that received alendronate before and after fracture compared with those with alendronate before fracture (j, $p = 0.053$). Genotypes are compared where indicated in A, B, C, and D and are pooled in E and F to compare treatment protocols.

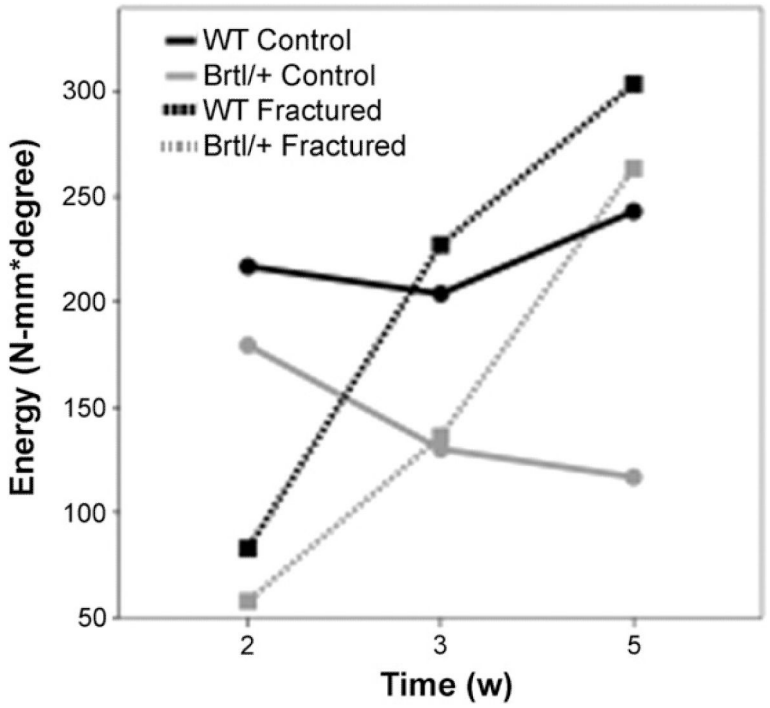

Fig. 5.

Mean energy to failure at various timepoints during healing for mice that did not receive alendronate. There was decreased energy to failure in both genotypes after 2 weeks of healing. After 5 weeks of healing, there was a statistically significant difference ($p < 0.05$) between the fractured and intact tibiae for Brtl/+ mice.

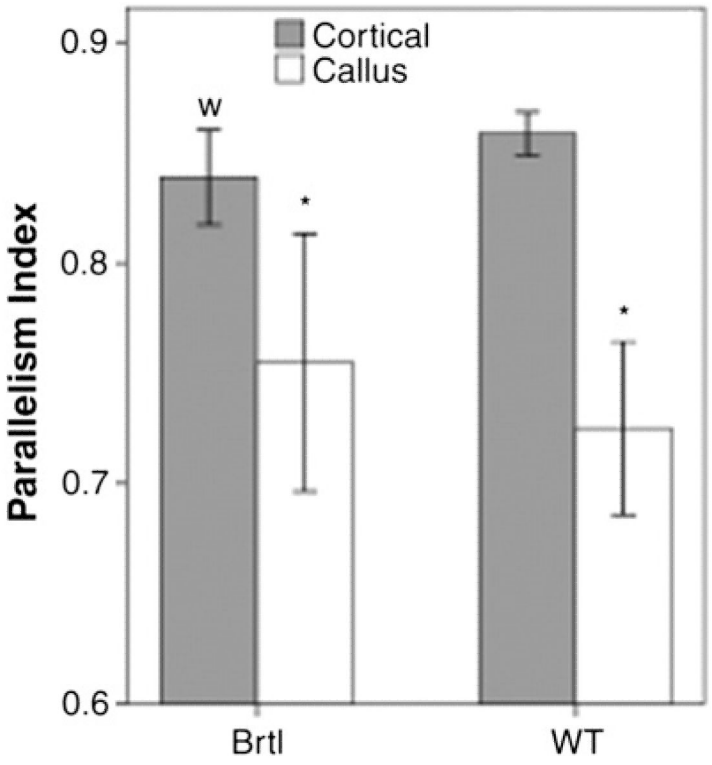

Fig. 6.

Parallelism index results for polarized light analysis after 5 weeks of healing. Notations indicate significance with respect to the cortical bone within a genotype (*, $p < 0.05$). For the cortical bone, there was no difference between the genotypes (w, $p = 0.072$).

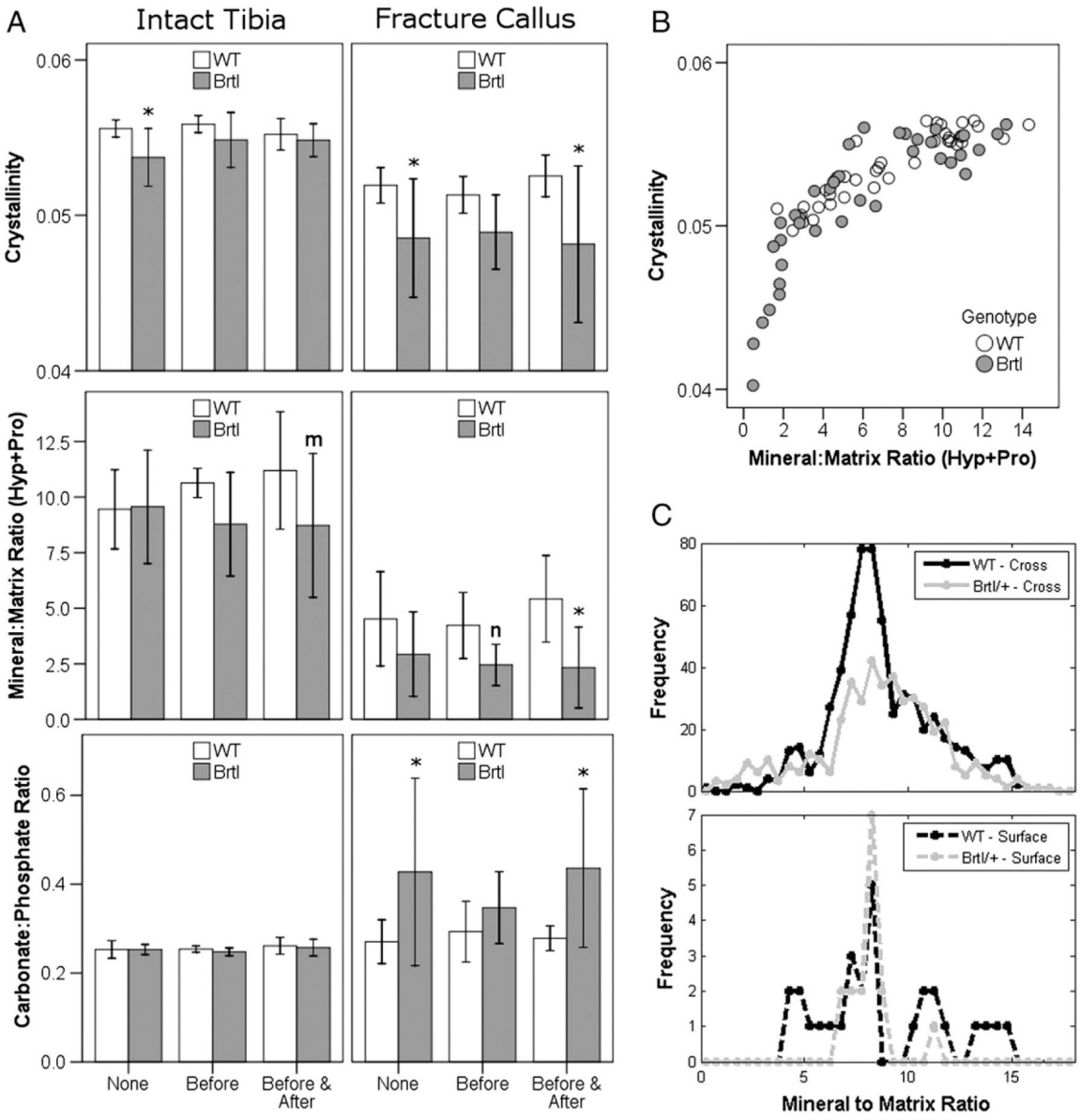

Fig. 7.

Raman microspectroscopy results. (A) Crystallinity (inverse full width at half height of 960 cm^{-1} peak), mineral-to-matrix ratio, and carbonate-to-phosphate ratio for intact tibiae and fracture callus at 3 weeks of healing. (B) Crystallinity vs. mineral-to-matrix ratio in both genotypes. In (C), histograms for spectra taken at the surface (bottom) appear to be a reasonable sampling of spectra taken through the cortical thickness (top). Notations indicate significance with respect to genotype (*, $p < 0.05$). No significant differences were found by genotype (m, $p = 0.076$ and n, $p = 0.075$) or between treatment groups.